

Estimating Sparse Networks with Hubs

Annaliza McGillivray¹, Abbas Khalili², and David A. Stephens²

¹Department of Mathematics and Statistics, University of Saskatchewan

²Department of Mathematics and Statistics, McGill University

July 10, 2022

Abstract

Graphical modelling techniques based on sparse selection have been applied to infer complex networks in many fields, including biology and medicine, engineering, finance and social sciences. One structural feature of some of the networks in such applications that poses a challenge for statistical inference is the presence of a small number of strongly interconnected nodes in a network which are called hubs. For example, in microbiome research hubs or microbial taxa play a significant role in maintaining stability of the microbial community structure. In this paper, we investigate the problem of estimating sparse networks in which there are a few highly connected hub nodes. Methods based on L_1 -regularization have been widely used for performing sparse selection in the graphical modelling context. However, while these methods encourage sparsity, they do not take into account structural information of the network. We introduce a new method for estimating networks with hubs that exploits the ability of (inverse) covariance selection methods to include structural information about the underlying network. Our proposed method is a weighted lasso approach with novel row/column sum weights, which we refer to as the hubs weighted graphical lasso. We establish large sample properties of the method when the number of parameters diverges with the sample size, and evaluate its finite sample performance via extensive simulations. We illustrate the method with an application to microbiome data.

KEY WORDS: Gaussian graphical model, Hubs, Sparsity, Weighted lasso.

1 INTRODUCTION

Over the past decade, fitting graphical models or networks via estimation of large sparse covariance and precision matrices has attracted much attention in modern multivariate analysis. Applications range from biology and medicine to engineering, economics, finance, and social sciences (Fan et al., 2016). To handle data scarcity in estimating large or high-dimensional sparse networks, methods based on L_1 -regularization (Meinshausen and Bühlmann, 2006; Yuan and Lin, 2007; Friedman et al., 2008) are widely used, the most popular being the graphical lasso (**glasso**) of Friedman et al. (2008). The **glasso** estimates the so-called precision matrix $\Theta = \Sigma^{-1}$ via maximizing an L_1 -penalized Gaussian log-likelihood, based on a random sample of p_n -dimensional Gaussian random vectors $\mathbf{X}_1, \dots, \mathbf{X}_n$ with mean $\mathbf{0}$ and covariance matrix Σ , (see Section 2). Under the Gaussianity assumption on $\mathbf{X}_i = (X_{i1}, X_{i2}, \dots, X_{ip_n})^\top$, a non-zero element θ_{jl} of Θ corresponds to an edge between two nodes X_{ij} and X_{il} in a graphical model for the data. The L_1 -penalty is applied to the non-diagonal elements of the presumably sparse precision matrix Θ . It is known that the **glasso** produces a sparse estimate of the precision matrix Θ . However, since the L_1 -penalty increases linearly in $|\theta_{jl}|$, the **glasso** also results in biased estimates of the large θ_{jl} . To reduce the estimation bias, Lam and Fan (2009) and Shen et al. (2012) proposed penalized likelihood approaches based on non-convex penalties such as smoothly clipped absolute deviation or SCAD (Fan and Li, 2001) for sparse precision matrix estimation and studied their theoretical properties; Fan et al. (2009) introduced the graphical adaptive lasso (Zou, 2006) to attenuate the bias problem in the network estimation.

Penalties such as L_1 and SCAD, however, implicitly assume that each potential edge in a network is equally likely and/or independent of all other edges (Tan et al., 2014), and may thus be inadequate for estimating networks with a few highly connected nodes, called *stars or hubs* (Figure 1). On the other hand, the weights in the graphical adaptive lasso (Fan et al., 2009) do not take network structural features such as hub nodes into consideration. In

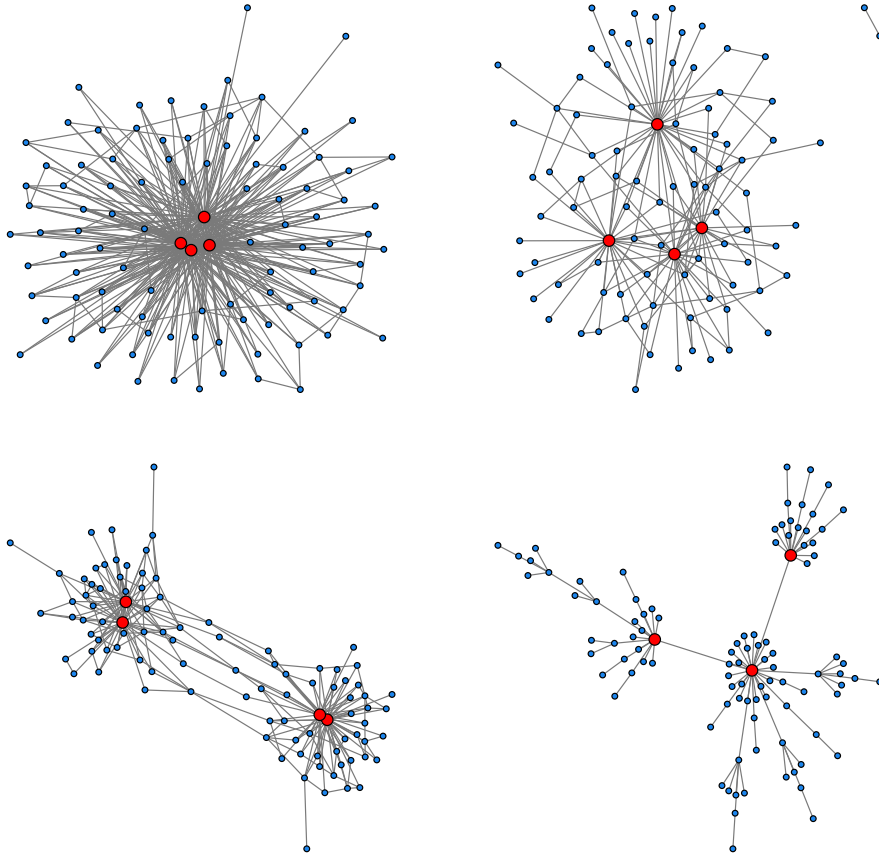


Figure 1: Simulated networks with hub nodes.

this paper, inspired by a microbiome data, we propose a new regularization method referred to as the hubs weighted graphical lasso for estimating sparse networks with a few hub nodes and in the presence of many low-degree nodes, when the dimension $p_n \rightarrow \infty$ as $n \rightarrow \infty$.

Rapidly developing sequencing technologies and analytical techniques have enhanced our ability to study the microorganisms such as bacteria, viruses, archaea and fungi that inhabit the human body (Gilbert et al., 2010) and a wide range of environments (Turnbaugh et al., 2007). The microorganisms inhabiting a particular environment do not exist in isolation, but interact with other microorganisms in a range of mutualistic and antagonistic relationships. One goal of microbiome studies is to model these microbial interactions from population-level data as a network reflecting co-occurrence and co-exclusion patterns between microbial taxa.

This is of interest not only for predicting individual relationships between microbes, but the structure of the interaction networks also gives insight into the organization of complex microbial communities. Friedman and Alm (2012) used networks of pairwise correlations between microbial taxa to model microbe-microbe interactions from microbial abundance data. However, correlation can be limiting in the multivariate setting as it is a pairwise measure of dependence. In addition, statistical challenges in studying networks of microbial interactions arise due to data scarcity and the organization of the network’s nodes into groups with different levels of connectivity. Specifically, microbial association networks tend to be sparse and also display *hubs* (van der Heijden and Hartmann, 2016). In ecology, these hubs can represent a few keystone species that are vital in maintaining stability of the microbial community (Kurtz et al., 2015).

To accommodate structural information such as hubs in network estimation, Tan et al. (2014) proposed the hubs graphical lasso (HGL), which is a penalization method that encourages estimates of the form $\widehat{\Theta}_n = \mathbf{Z} + \mathbf{V} + \mathbf{V}^\top$, where \mathbf{Z} is a sparse symmetric matrix capturing edges between non-hub nodes and \mathbf{V} is a matrix whose columns are either entirely zero or almost entirely non-zero with the non-zero elements of \mathbf{V} representing hub edges. The HGL applies an L_1 -penalty to the off-diagonal elements of \mathbf{Z} , and L_1 and group lasso (Yuan and Lin, 2007) penalties to the columns of \mathbf{V} . The method requires proper choices of three tuning parameters that are present in the L_1 -penalized likelihood and are selected by a BIC-type quantity. The HGL is specifically designed for networks with dense hub nodes, referred to as super hubs. Liu and Ihler (2011) proposed a method for estimating scale-free networks, which are characterized as having a degree distribution that follows a power law. Their method is, in particular, a re-weighted L_1 -regularization approach, where the weights in the iterative procedure are updated in a rich-get-richer fashion, mimicking the generating mechanism of scale-free networks (Barabási and Albert, 1999). Such an approach, however, cannot model super hubs (Tan et al., 2014). Hero and Rajaratnam (2012) proposed a screening method for hub screening in high dimensions but it does not estimate the edges of the network.

In this paper, we introduce a new approach for estimating networks with hubs that exploits the ability of (inverse) covariance selection methods to include structural information about the underlying network, and can accommodate both networks with so-called super hubs as well as scale-free networks. More specifically, our method called the hubs weighted graphical lasso (**hw.glasso**), is a weighted graphical lasso approach with novel informative row/column sum weights that allow for differential penalization of hub edges compared to non-hub edges. We show that the **hw.glasso** estimator is both estimation and selection consistent, when $p_n \rightarrow \infty$ as $n \rightarrow \infty$. Our theoretical development applies to a general weighted graphical lasso approach including the adaptive graphical lasso (Fan et al., 2009). We also demonstrate that, unlike L_1 -penalty, in order to achieve the aforementioned theoretical properties we do not need a restriction of the form $O(1)$ or $O(p_n)$ on the number of true non-zero elements of Θ_0 (Lam and Fan, 2009). In practice, the **hw.glasso** leads to an optimization problem that is solved using the efficient graphical lasso algorithm of Friedman et al. (2008), already implemented in the R package **glasso**. Via extensive simulations, we show that the method performs well in finite sample situations that we have considered here.

The remainder of this paper is organized as follows. In Section 2, we introduce the penalized likelihood problem and commonly used penalty functions in the context of performing sparse inverse covariance estimation. In Section 3, we present the hubs weighted graphical lasso estimator, and investigate its theoretical properties in Section 4. We then assess its finite sample performance through simulation studies in Section 5, and with an application to two microbiome data sets in Section 6. We conclude with a discussion in Section 7. The proof of our main theoretical result is provided in the Appendix.

2 PROBLEM SETUP

Suppose $\mathbf{X}_1, \dots, \mathbf{X}_n$ are p_n -dimensional independent and identically distributed (i.i.d.) random vectors from a Gaussian distribution with mean $\mathbf{0}$ and covariance matrix $\Sigma = \Theta^{-1}$, and let $\mathbf{x}_1, \dots, \mathbf{x}_n$, with $\mathbf{x}_i = (x_{i1}, \dots, x_{ip_n})^\top$, denote realizations of the random variables. Further, denote the sample covariance matrix by S_n , where $S_n = \sum_{i=1}^n \mathbf{x}_i \mathbf{x}_i^\top / n$. Then the

re-scaled log-likelihood function of Θ (up to a constant) is given by

$$\ell_n(\Theta) = \log \det \Theta - \text{tr}(S_n \Theta), \quad (1)$$

where $\text{tr}(\cdot)$ denotes the trace. For a sparse Gaussian graphical model, the precision matrix Θ is estimated by the maximizer of the penalized log-likelihood function

$$pl_n(\Theta) = \ell_n(\Theta) - p_{\lambda_n}(\Theta), \quad (2)$$

where $p_{\lambda_n}(\cdot)$ is a generic penalty function on Θ with tuning parameter $\lambda_n > 0$.

Friedman et al. (2008) considered the L_1 -penalty function $p_{\lambda_n}(\Theta) = \lambda_n \sum_{i < j} |\theta_{ij}|$ in (2) and proposed the graphical lasso algorithm that makes use of a block coordinate descent procedure to optimize (2). Lam and Fan (2009) studied nonconvex penalties such as the SCAD in (2). While these penalties induce sparsity in the estimated Θ , they do so by penalizing the elements of Θ equally and/or independently of each other. One penalty function that allows for varying levels of penalization to the θ_{ij} is the adaptive lasso (Zou, 2006; Fan et al., 2009), given by $p_{\lambda_n}(\Theta) = \lambda_n \sum_{i < j} \tilde{w}_{ij} |\theta_{ij}|$, where $\tilde{w}_{ij} = 1/|\tilde{\theta}_{ij}|^\gamma$ for some $\gamma > 0$ and any consistent estimate $\tilde{\Theta}_n = (\tilde{\theta}_{ij})_{i,j=1}^{p_n}$ of Θ . While these choices of the penalty result in a sparse estimate of Θ and lead to desirable asymptotic properties (Lam and Fan, 2009), they do not incorporate any prior information of structural features such as hub nodes in the precision matrix. This motivated us to propose a method that allows for the inclusion of such rich structural information in the penalty function in (2).

3 HUBS WEIGHTED GRAPHICAL LASSO

When the true underlying Gaussian graphical model has hub nodes (see Figure 1), we wish to incorporate into our estimation procedure not merely sparsity, but the knowledge of the presence of these highly connected nodes. In this section, we present a new penalty function in (2) that utilizes this knowledge.

Since the true underlying graph has hub nodes, in the precision matrix Θ the rows/columns corresponding to each hub node are significantly denser (i.e., have more non-zero elements) than those corresponding to the non-hub nodes. In Figure 1, we display four different types

of networks with hubs, from top-left to bottom-right: the first, illustrates a network with so-called “super hubs”, while the second and third display networks with hubs that are less densely connected than the “super hubs” in the first, and the fourth displays a scale-free network (Barabási and Albert, 1999).

To estimate networks with hubs, we adopt a new weighted lasso approach that uses informative weights based on row/column sums of the precision matrix. In what follows, we outline our proposed estimation procedure by first introducing the new weights.

Let $\tilde{\Theta}_n = (\tilde{\theta}_{ij})_{i,j=1}^{p_n}$ be any consistent estimator of the precision matrix Θ . Depending on the dimension p_n , we may take $\tilde{\Theta}_n$ to be the inverse of the sample covariance matrix S_n , or use the precision matrix estimate obtained from the graphical lasso (Friedman et al., 2008). We then construct the symmetric matrix $\tilde{W}_n = (\tilde{w}_{ij})_{i,j=1}^{p_n}$ of weights

$$\tilde{w}_{ij} = \frac{1}{|\tilde{\theta}_{ij}|^{\gamma_1} \left(\|\tilde{\theta}_{-i}\|_1 \cdot \|\tilde{\theta}_{-j}\|_1 \right)^{\gamma_2}} \quad , \text{ if } i \neq j \quad (3)$$

and $\tilde{w}_{ij} = 0$ if $i = j$, for some $\gamma_1, \gamma_2 > 0$, where $\tilde{\theta}_{-i} = \left\{ \tilde{\theta}_{ik} : k = 1, \dots, p_n, k \neq i \right\}$ is the i^{th} row (or by symmetry, the i^{th} column) of $\tilde{\Theta}_n$, and $\|\tilde{\theta}_{-i}\|_1 = \sum_{k \neq i} |\tilde{\theta}_{ik}|$.

We now define the hubs weighted graphical lasso (**hw.glasso**) estimator $\hat{\Theta}_n$ of Θ to be

$$\hat{\Theta}_n = \arg \max_{\Theta > 0} \left\{ \ell_n(\Theta) - \lambda_n \|\tilde{W}_n * \Theta\|_1 \right\}, \quad (4)$$

where $\lambda_n > 0$ is a tuning parameter, and $*$ is the Schur matrix product so that

$$\|\tilde{W}_n * \Theta\|_1 = \sum_{i < j} \tilde{w}_{ij} |\theta_{ij}|. \quad (5)$$

The weights \tilde{w}_{ij} are designed to allow for less penalization of hub edges compared to non-hub edges. More specifically, if nodes i and j are hubs, then both $\sum_{k \neq i} |\tilde{\theta}_{ik}|$ and $\sum_{k \neq j} |\tilde{\theta}_{kj}|$ should be large and thus the weight \tilde{w}_{ij} will be small. If either nodes i or j are hubs, then one of $\sum_{k \neq i} |\tilde{\theta}_{ik}|$ and $\sum_{k \neq j} |\tilde{\theta}_{kj}|$ should be large and thus the weight \tilde{w}_{ij} will be moderately sized. If neither nodes i nor j are hubs, then both $\sum_{k \neq i} |\tilde{\theta}_{ik}|$ and $\sum_{k \neq j} |\tilde{\theta}_{kj}|$ should be small and so the weight \tilde{w}_{ij} will be large. The additional term $|\tilde{\theta}_{ij}|^{\gamma_1}$ in the weights induces sparsity by allowing for zero entries in rows (columns) corresponding to hubs.

The proposed approach belongs to the family of weighted graphical lasso methods that allow for different penalties on the entries of Θ , which includes the graphical adaptive lasso (Fan et al., 2009). Weighted lasso approaches can result in less bias than the standard lasso by adapting penalties to incorporate information about the location of zeros, based on either an initial estimate or background knowledge.

Numerical Algorithm:

The advantage of the `hw.glasso` method is that it leads to the optimization problem (4) that can be solved using the efficient graphical lasso algorithm of Friedman et al. (2008), already implemented in the R package `glasso`. In their implementation, the user may specify a symmetric weight matrix, which in our case is \widetilde{W}_n defined in (3). For the choice of the tuning parameter λ_n , we employ the Bayesian information criterion (BIC) which has been widely used in the literature (e.g. Gao et al., 2012). In our simulation studies and real data analysis respectively in Sections 5 and 6, we take $\gamma_1 = \gamma_2 = 1$.

4 THEORETICAL PROPERTIES

In this section, we first view the estimator $\widehat{\Theta}_n$ in (4) as a general weighted `glasso` estimator and derive conditions on the weights \widetilde{w}_{ij} in (5) that guarantee consistency and sparsistency (see below) of $\widehat{\Theta}_n$. We then focus on the specific weights (3) that resulted in our hubs estimator `hw.glasso`. In general, the weights \widetilde{w}_{ij} depend on the sample size n and are possibly random.

We assume that $\mathbf{X}_1, \dots, \mathbf{X}_n$ are p_n -dimensional i.i.d. Gaussian random vectors with mean $\mathbf{0}$ and true covariance matrix Σ_0 . The corresponding true sparse precision matrix is $\Sigma_0^{-1} = \Theta_0 = (\theta_{ij}^0)_{i,j=1}^{p_n}$, where the dimension p_n tends to infinity at a certain rate to be later specified, as $n \rightarrow \infty$. First, we introduce some notation and state certain regularity conditions on the true precision matrix $\Theta_0 = (\theta_{ij}^0)$.

We define $T = \{(i, j) : \theta_{ij}^0 \neq 0, i < j\} \neq \emptyset$ to be the set of indices of all non-zero off-diagonal elements in Θ_0 and let $q_n = |T|$ be the cardinality of T . The set of indices of the true zero elements of Θ_0 is denoted by T^c . Let $\phi_{\min}(A)$ and $\phi_{\max}(A)$ denote the minimum and

maximum eigenvalues of a matrix A . Further, let $\|A\|_F^2 = \text{tr}(A^\top A)$ and $\|A\|^2 = \phi_{\max}(A^\top A)$ be the Frobenius and operator norms of A , respectively. Also, recall from (3) that $\|\boldsymbol{\theta}_{-i}^0\|_1 = \sum_{k \neq i} |\theta_{ik}^0|$. We assume that the following regularity conditions hold.

Condition 1: There exist constants τ_1 and τ_2 such that $0 < \tau_1 \leq \phi_{\min}(\Theta_0) < \phi_{\max}(\Theta_0) \leq \tau_2 < \infty$.

Condition 2: There exists a constant $\tau_3 > 0$ such that $\min_{(i,j) \in T} |\theta_{ij}^0| \geq \tau_3$.

Condition 1 guarantees the existence of the inverse Θ_0 . Condition 2 is a signal strength assumption; it ensures that the non-zero elements of Θ_0 are bounded away from zero. The proofs of our results are given in the Appendix. Our first result concerns the estimation *consistency* of the weighted **glasso** estimator.

Theorem 1 (*Consistency*) *Suppose Conditions 1 and 2 hold, and $(p_n + q_n)(\log p_n)/n = o(1)$. Further, assume that λ_n and \tilde{w}_{ij} are chosen such that $\lambda_n \max_{(i,j) \in T} \tilde{w}_{ij} = O_p(\{(\log p_n)/n\}^{1/2})$ and $\{(\log p_n)/n\}^{1/2} \{\min_{(i,j) \in T^c} \tilde{w}_{ij}\}^{-1} = O_p(\lambda_n)$. Then the weighted **glasso** estimator $\hat{\Theta}_n$ satisfies*

$$\|\hat{\Theta}_n - \Theta_0\|_F = O_p \left[\left\{ \frac{(p_n + q_n) \log p_n}{n} \right\}^{1/2} \right]. \quad (6)$$

Theorem 1 shows that with the proper choice of the tuning parameter λ_n and the weights \tilde{w}_{ij} , $\hat{\Theta}_n$ is a consistent estimator of Θ_0 . For example, if the (possibly random) weights are chosen such that $\max_{(i,j) \in T} \tilde{w}_{ij} \rightarrow C_1 < \infty$ and $\min_{(i,j) \in T^c} \tilde{w}_{ij} \rightarrow \infty$ (in probability), as $n \rightarrow \infty$, then the choice $\lambda_n = C_2 \{(\log p_n)/n\}^{1/2}$, for some finite constant $C_2 > 0$, results in consistency of $\hat{\Theta}_n$. As pointed out by Rothman et al. (2008) and Lam and Fan (2009), the worst part of the rate of convergence of $\hat{\Theta}_n$ in (6) is the term $p_n \log p_n/n$, which is due to the estimation of p_n diagonal elements of Θ_0 . The effect of diverging dimensionality is reflected by the term $\log p_n$.

Our next result establishes that the weighted **glasso** estimates the true zero entries of the precision matrix as zero with probability tending to 1. This property is referred to as *sparsistency* in Lam and Fan (2009).

Theorem 2 (*Sparsistency*) Assume the conditions of Theorem 1 are fulfilled, and that

$$\|\widehat{\Theta}_n - \Theta_0\|^2 = O_p(\eta_n) \quad (7)$$

for a sequence η_n such that $\eta_n \rightarrow 0$ and $\{\min_{(i,j) \in T^c} \widetilde{w}_{ij}\}^{-2} \eta_n = O_p(\lambda_n^2)$. Then the weighted **glasso** estimator $\widehat{\Theta}_n$ has the property $P(\widehat{\theta}_{ij} = 0 : (i, j) \in T^c) \rightarrow 1$, as $n \rightarrow \infty$.

The two theorems provide general conditions on the weights \widetilde{w}_{ij} , and (λ_n, η_n) , that guarantee consistency and sparsistency of the weighted **glasso** estimator. In this paper, we focus on the specific weights \widetilde{w}_{ij} in (3) which are used in our hubs weighted graphical lasso (**hw.glasso**) estimator. These weights are constructed using the popular **glasso** estimator $\widetilde{\Theta}_n$. Proposition 1 below verifies conditions of the theorems on such weights.

Proposition 1 Consider the **hw.glasso** estimator $\widehat{\Theta}_n$ with the specific weights \widetilde{w}_{ij} in (3).

The estimator has consistency property (6) if $\{\lambda_n, p_n, q_n\}$ satisfy

$$\lambda_n = O(\sqrt{\log p_n/n}), \quad \left(\frac{\log p_n}{n}\right)^{1/2} \left\{ \frac{(p_n + q_n) \log p_n}{n} \right\}^{\gamma_1/2} \lambda_n^{-1} = O(1). \quad (8)$$

The estimator has also sparsistency property if we have (8), and (7) with η_n satisfying

$$\sqrt{\eta_n} \left(\frac{(p_n + q_n) \log p_n}{n} \right)^{\gamma_1/2} \lambda_n^{-1} = O(1). \quad (9)$$

It is worth noticing that the exponent γ_2 in (3) does not play a role in the asymptotic properties of the **hw.glasso** estimator, whereas γ_1 does. In other words, the **hw.glasso** estimator has similar asymptotic properties as the graphical adaptive lasso (Fan et al., 2009) estimator which uses the weights in (3) with $\gamma_1 > 0$ and $\gamma_2 = 0$. However, as demonstrated in our simulations, their finite sample performance may be very different, due to the presence of $\gamma_2 > 0$ in the weights (3) used for the **hw.glasso** estimator which is designed for networks with hubs. We investigate finite sample performance of different estimators in Section 5.

We now discuss the rate η_n in (7). Note that for any $m \times m$ matrix A , we have that $\|A\|^2 \leq \|A\|_{\mathbb{F}}^2 \leq m \|A\|^2$. Let $r_n = \sqrt{(p_n + q_n) \log p_n/n}$. Under (8), the **hw.glasso** estimator

$\widehat{\Theta}_n$ satisfies (6) and thus $\|\widehat{\Theta}_n - \Theta_0\|^2 \leq r_n^2 \leq p_n \|\widehat{\Theta}_n - \Theta_0\|^2$. If we consider the worst case scenario that $\eta_n = r_n^2$, then the sparsistency condition (9) becomes

$$\left\{ (p_n + q_n)^{\gamma_1+1} \left(\frac{\log p_n}{n} \right)^{\gamma_1} \right\}^{1/2} = O(1). \quad (10)$$

On the other hand, in the optimistic scenario that $\eta_n = r_n^2/p_n$, condition (9) becomes

$$\sqrt{\frac{(p_n + q_n)}{p_n}} \left(\frac{(p_n + q_n) \log p_n}{n} \right)^{\gamma_1/2} = O(1). \quad (11)$$

Thus, under the above two scenarios, the `hw.glasso` estimator $\widehat{\Theta}_n$ does not have the limitations of the forms $O(1)$ or $O(p_n)$ for the sparsity factor q_n as discussed in Lam and Fan (2009) for the standard L_1 estimator. In other words, as long as (10) or (11) are satisfied, $\widehat{\Theta}_n$ has sparsistency property.

5 NUMERICAL RESULTS

In this section, we compare via simulation the finite-sample performance of our proposed `hw.glasso` procedure to the graphical lasso (`glasso`; Friedman et al., 2008), the graphical adaptive lasso (`Ada-glasso`) (Fan et al., 2009), the scale-free (`SF`) network estimation procedure of Liu and Ihler (2011), and the hubs graphical lasso (`HGL`) of Tan et al. (2014). We also provide simulation results for a two-step `hw.glasso` procedure, introduced in Section 5.2, in the case where the hubs are *unknown*, but also in the case where the hubs are *known* which is a reasonable assumption in some biological applications.

To implement the graphical (adaptive) lasso and our method, we use the R function `glasso` and select the tuning parameter λ from a fine grid based on BIC, and we set $\gamma_1 = \gamma_2 = 1$. To implement `HGL`, we use the R package `hglasso`. Each tuning parameter ρ_i for $i = 1, 2, 3$ in `HGL` is selected from a fine grid. We also consider various values of c in the BIC-type quantity in Tan et al. (2014).

5.1 Performance Measures and Simulation Settings

We now provide the performance measures by which various procedures are assessed as well as the simulation settings under consideration. We first introduce some notation.

Let TP, TN, FP and FN denote the numbers of true positives (true non-zero θ_{ij}^0 's), true negatives (true zero θ_{ij}^0 's), false positives, and false negatives, respectively. Further, let \mathcal{H} denote the set of indices of true hub nodes, $\widehat{\mathcal{H}}$ the set of indices of estimated hub nodes, and $|\mathcal{H}|$ denote the size of the set \mathcal{H} . To assess the hub structure recovery performance of each of the methods, we consider a node to be a hub if it is connected to more than $k\%$ of all other nodes. The methods are evaluated using the following empirical measures:

- True negative rate (TNR, specificity): $\text{TNR} = \frac{\text{TN}}{\text{TN} + \text{FP}} = \frac{\sum_{i < j} I(\widehat{\theta}_{ij} = 0, \theta_{ij}^0 = 0)}{\sum_{i < j} I(\theta_{ij}^0 = 0)}$
- True positive rate (TPR, sensitivity): $\text{TPR} = \frac{\text{TP}}{\text{TP} + \text{FN}} = \frac{\sum_{i \leq j} I(\widehat{\theta}_{ij} \neq 0, \theta_{ij}^0 \neq 0)}{\sum_{i \leq j} I(\theta_{ij}^0 \neq 0)}$
- Percentage of correctly estimated hub edges: $\frac{\sum_{i \in \mathcal{H}, i \neq j} I(\widehat{\theta}_{ij} \neq 0, \theta_{ij}^0 \neq 0)}{\sum_{i \in \mathcal{H}, i \neq j} I(\theta_{ij}^0 \neq 0)} \times 100\%$
- Percentage of correctly estimated hub nodes: $\frac{|\widehat{\mathcal{H}} \cap \mathcal{H}|}{|\mathcal{H}|} \times 100\%$
- Percentage of correctly estimated non-hub nodes: $\frac{|\widehat{\mathcal{H}}^c \cap \mathcal{H}^c|}{|\mathcal{H}^c|} \times 100\%$, where $\widehat{\mathcal{H}}^c = \{1, \dots, p\} \setminus \widehat{\mathcal{H}}$
- Frobenius norm: $\frac{1}{p} \|\widehat{\Theta} - \Theta_0\|_F^2 = \frac{1}{p} \sum_{i \neq j} (\widehat{\theta}_{ij} - \theta_{ij}^0)^2$,

where $\widehat{\Theta} = (\widehat{\theta}_{ij})_{i,j=1}^p$ is the estimated precision matrix, and $\Theta_0 = (\theta_{ij}^0)_{i,j=1}^p$ represents the true underlying precision matrix (network). Averages (and standard errors) of these performance measures over 100 replications are reported in Tables 1 to 4.

We consider four generating mechanisms for the adjacency matrix A of the network, similar to those in Tan et al. (2014):

- (i) We randomly select the set \mathcal{H} of true hub nodes and set the elements of the corresponding rows/columns of the adjacency matrix A equal to 1 with probability 0.8 and 0 otherwise. Next, we set $A_{ij} = A_{ji} = 1$ for all $i < j$ with probability 0.01, and 0 otherwise.

- (ii) We use the same setup as in (i) except that, to generate the adjacency matrix A , each hub node is connected to another node with probability 0.3.
- (iii) The adjacency matrix is $A = \begin{pmatrix} A_1 & B \\ B^T & A_2 \end{pmatrix}$, where A_1 and A_2 are generated as in (i), except that all nodes have a connection probability of 0.04, and $B = (b_{ij})$ has $b_{ij} = 1$ with probability 0.01 and $b_{ij} = 0$ otherwise.
- (iv) Scale-free networks: for a scale-free network, the probability that a node has degree d follows a power law distribution $P(d) \sim d^{-\alpha}$. Such a network is generated using the Barabási and Albert (1999) algorithm that incorporates growth and preferential attachment, which are two mechanisms that are common to a number of real-world networks, such as business networks and social networks. We use the R package `igraph` to generate scale-free networks with $\alpha = 2$. Note that the hub nodes in this simulation are less densely connected than those in Simulations (i)-(iii).

For each of the adjacency matrices in (i)-(iv), we then construct a symmetric matrix Ω such that $\Omega_{ij} = 0$ if $A_{ij} = 0$, and Ω_{ij} are independent from the uniform distribution on $[-0.8, -0.5] \cup [0.5, 0.8]$ if $A_{ij} = 1$. Finally, we take $\Theta = \Omega + \{0.1 - \lambda_{\min}(\Omega)\} I_p$, where $\lambda_{\min}(\Omega)$ is the smallest eigenvalue of Ω , to ensure that all eigenvalues of Θ are positive. For Simulations (i) and (ii), we take the number of hubs to be $|\mathcal{H}| = \lfloor p/25 \rfloor$. The simulated networks for $p = 100$ are displayed in Figure 1. When evaluating the performance of each of the methods, we consider a node to be a hub if it is connected to more than $k = 10\%$ of all other nodes. Note that for Simulations (i)-(iii), there is a clear distinction between hubs and non-hubs, but the cutoff threshold of 10% is needed to distinguish a hub from a non-hub in scale-free networks, generated for Simulation (iv).

5.2 A Two-Step Hubs Weighted Graphical Lasso

In our simulation studies, we observe that finite-sample performance of the proposed `hw.glasso` can be improved by first identifying a set of candidate hubs $\widehat{\mathcal{H}}$ based on the

`hw.glasso` estimate $\widehat{\Theta}_n$ and then penalizing the hub edges separately from the non-hub edges through a second weighted graphical lasso. In what follows, we outline this 2-step `hw.glasso` approach.

Based on the `hw.glasso` estimate $\widehat{\Theta}_n$, defined in (4), we identify a set of candidate hubs $\widehat{\mathcal{H}}$ (see the Remarks below for the choice of $\widehat{\mathcal{H}}$). We then construct a symmetric weight matrix $\widehat{W} = (\widehat{w}_{ij})$, where

$$\widehat{w}_{ij} = \begin{cases} \lambda_1 & \text{if } i \in \widehat{\mathcal{H}} \text{ or } j \in \widehat{\mathcal{H}}, i \neq j \\ \lambda_2 & \text{if } i, j \notin \widehat{\mathcal{H}}, i \neq j \\ 0 & \text{if } i = j \end{cases}$$

for some tuning parameters $\lambda_1, \lambda_2 > 0$, and solve the weighted lasso optimization problem

$$\bar{\Theta}_n = \arg \max_{\Theta > 0} \left\{ \log \det \Theta - \text{tr}(S_n \Theta) - \|\widehat{W} * \Theta\|_1 \right\},$$

where we refer to $\bar{\Theta}_n$ as the 2-step `hw.glasso` estimator of Θ . The tuning parameter λ_1 controls the number of edges connecting a hub node to any other node in the graph, while the tuning parameter λ_2 controls the number of edges connecting two non-hub nodes. In our simulation studies, λ_1 and λ_2 are chosen using BIC.

Remarks:

Here we discuss two possible approaches for identifying a set of candidate hubs $\widehat{\mathcal{H}}$ based on the one-step `hw.glasso` estimate $\widehat{\Theta}_n$:

- (a) The set $\widehat{\mathcal{H}}$ can be obtained by setting a cutoff threshold for a node to be a hub. For example, as mentioned in Section 5.1, we classify a node as a hub if it is connected to more than 10% of all other nodes.
- (b) The set $\widehat{\mathcal{H}}$ can also be obtained by using a clustering approach. From the first-step estimate $\widehat{\Theta}_n$, the degree of each node is computed and K-means clustering is then applied to cluster the nodes into two groups, where the hub group is characterized

as the group with the larger mean degree. A similar approach based on a two-component Gaussian mixture model was considered by Charbonnier et al. (2010) in order to cluster nodes in a *directed* graph as hubs and leaves.

5.3 Discussion of Simulation Results

From Tables 1 to 3 corresponding to Simulations (i) to (iii), respectively, we see that when the true underlying network has hubs, the one-step `hw.glasso` procedure results in substantially better finite-sample performance compared to `glasso` and `Ada-glasso` that do not explicitly take hub structure into account. The `hw.glasso` procedure also outperforms the HGL and SF which are methods designed specifically for modelling networks with hubs. For Simulations (ii) and (iii) in which the hubs are not as highly connected, `hw.glasso` and `Ada-glasso` perform similarly when $n > p$, but the performance of `hw.glasso` increasingly improves relative to `Ada-glasso` as p increases. The SF approach does not result in significant improvements over the `glasso` and `Ada-glasso` procedures, which is expected as it is not designed for estimating networks with very densely connected hubs. The HGL tends to perform better than `glasso` and `Ada-glasso` in terms of hub edge identification. However, with $c = 0.5$ and $c = 0.75$, which is a user-specified tuning parameter in the BIC-type quantity of Tan et al. (2014), HGL leads to much denser graphs compared to `glasso`. The tuning parameter c controls the number of hubs in the graph, favouring more hubs when c is small.

Results of the 2-step `hw.glasso` procedures are also provided in Tables 1 to 3. We see that when the true hubs are known in advance, which is a reasonable assumption in some biological applications, the 2-step `hw.glasso` that takes into account knowledge of these hubs results in significant improvements over the competing methods listed in the tables. While the 2-step `hw.glasso` in the case where the hubs are unknown performs better in higher dimensions than the one-step version, the 2-step procedure requires setting a cutoff threshold for a node to be considered a hub.

The results for Simulation (iv) are given in Table 4. Note that the scale-free networks generated in this simulation have hubs that are not as highly connected as those in Simulations

(i)-(iii). From Table 4, it is thus not surprising that **Ada-glasso** performs well. When $p \geq n$, knowing the true hubs in advance and allowing for different levels of penalization between hub and non-hub edges, the 2-step **hw.glasso** results in better performance compared to the other methods across almost all performance measures. The one-step **hw.glasso** procedure performs well in terms of hub edge identification. The results for **HGL** are omitted as their method is not designed for estimating scale-free networks.

6 REAL DATA EXAMPLE

In this section, we illustrate the proposed methodology by estimating microbial interaction networks using undirected graphical models. The analysis is based on saliva microbiome relative abundance data sets of two *Pan* species found in Li et al. (2013). We use relative abundances of genera in the saliva microbiomes of 23 bonobos (*Pan paniscus*) from the Lola ya Bonobo Sanctuary in the Democratic Republic of the Congo, and 22 chimpanzees (*Pan troglodytes*) from the Tacugama Chimpanzee Sanctuary in Sierra Leone.

For the bonobos, 69 genera were identified along with 2 unknown/unclassified genera. *Enterobacter* (20.8%) was the most abundant genus identified, followed by *Porphyromonas* (10.3%) and *Neisseria* (9.7%). For the chimpanzees, 79 genera were identified along with 2 unknown/unclassified genera. The most abundant genera identified were *Porphyromonas* (16.9%), *Fusobacterium* (14.0%), *Haemophilus* (11.4%) and *Neisseria* (8.1%).

As microbial relative abundance data are compositional, after replacing zero abundance counts by 0.5, we use a centered log-ratio transformation (Aitchison, 1981) of the data for our analysis. We then estimate undirected graphical models for each data set, using the **Ada-glasso** and **hw.glasso** procedures. We select the tuning parameter λ from a fine grid using BIC, and set $\gamma_1 = \gamma_2 = 1$. To obtain a graph that is reproducible under random sampling, we generate 100 bootstrap samples and repeat the **hw.glasso** procedure on each sample. The stability of the network is then measured by the average proportion of edges reproduced by each bootstrap replicate. Only the edges that are reproduced in at least 80% of the bootstrap replicates are retained in the final network.

Assuming hub structures for both the bonobo and chimpanzee microbial interaction networks and applying the `hw.glasso` procedure (retaining only reproducible edges), we found nodes corresponding to genera *Actinobacillus*, *Enterobacter* and *Escherichia* to be highly connected for the bonobo group, and the node corresponding to genus *Prevotella* to be highly connected for the chimpanzee group. There are 58 edges that are common between the two groups. For both groups, there is a tendency for genera to correlate positively with other genera from the same phylum, especially within *Proteobacteria* and *Firmicutes*, which was also found in Li et al. (2013).

For each network, we use the R package `igraph` to evaluate several network measures, including network density, global clustering coefficient, betweenness centrality, and average path length. Differences in network measures between the bonobo and chimpanzee groups are assessed for statistical significance by permutation tests with 1000 randomizations. More specifically, we randomly assign the apes to one of two groups 1000 times. For each permutation, a network is estimated for each group and distributions of the differences in network indices are generated for statistical inference. No significant differences were found in terms of the global network structure (measured by global clustering coefficient, betweenness centrality and average path length) between the two groups. Significant differences in degree centrality were found for nodes corresponding to genera *Escherichia* (0.35 v 0.14, $p = 0.03$) and *Peptostreptococcaceae* (0.02 v 0.18, $p = 0.04$).

The networks produced by our proposed method are displayed in Figures 2 and 3. The hubs identified by our method were found to be the highest connected nodes by the `Ada-glasso`, but our procedure assigned more edges to hubs and fewer edges to non-hubs, compared to the `Ada-glasso`.

7 DISCUSSION

In this paper, we proposed a new weighted graphical lasso approach for estimating networks with hubs that makes use of informative weights that allow for hub structure. We showed that the proposed method, referred to as the hubs weighted graphical lasso

(`hw.glasso`), is both estimation and selection consistent. We then demonstrated with simulated data that the proposed method performs significantly better than methods that do not explicitly take hub structure into account, but it also outperforms network estimation procedures designed for modelling networks with hubs, such as the HGL of Tan et al. (2014) and the re-weighted L_1 -regularization approach of Liu and Ihler (2011). The former is designed for estimating networks with very densely connected hub nodes, referred to as “super hubs”, while the latter is designed for estimating scale-free networks, for which there may be no clear distinction between *hub* and *non-hub* nodes. Our proposed method can accommodate both networks with so-called “super hubs” as well as scale-free networks.

This work focuses on the problem of static network modelling, where the inferred network may provide a snapshot of a network structure at a single time point. In some applications, networks may undergo changes over time in response to changes in external conditions and the temporal variation of these networks can be captured by dynamic networks (Faust et al., 2015). Techniques developed for static network modelling will pave the way for proposing new approaches for modelling the dynamics of networks with hubs.

APPENDIX: PROOFS

Let $A^+ = \text{diag}(A)$ be a diagonal matrix with the diagonal elements of a matrix A , and further let $A^- = A - A^+$. Also, for any two matrix $B_{m \times m} = \{b_{ij}\}$ and $C_{n \times n} = \{c_{kl}\}$, their Kronecker product $B \otimes C = \{b_{ij}c_{kl}\}$. For any closed bounded convex set \mathcal{C} which contains $\mathbf{0}$, its boundary is denoted by $\partial\mathcal{C}$. Finally, recall from (3) that $\|\boldsymbol{\theta}_{-i}^0\|_1 = \sum_{k \neq i} |\theta_{ik}^0|$. We also use the result of Lemma 3 of Bickel and Levina (2008), re-stated in what follows.

Lemma 1 *Let $\mathbf{X}_i = (X_{i1}, X_{i2}, \dots, X_{ip})^\top, i = 1, 2, \dots, n$, be i.i.d from Gaussian with mean $\mathbf{0}$ and covariance matrix $\boldsymbol{\Sigma}_0 = \{\sigma_{ij}^0\}$ such that $\phi_{\max}(\boldsymbol{\Sigma}_0) \leq \tau_1^{-1} < \infty$, then*

$$P \left[\left| \sum_{i=1}^n (X_{ij}X_{ik} - \sigma_{ij}^0) \right| \geq n\nu \right] \leq c_1 \exp(-c_2 n\nu^2) \quad , \quad |\nu| \leq \delta,$$

where c_1, c_2 and δ depend on τ_1 only.

We now proceed with the proof of our first result.

Proof of Theorem 1: The idea of the proof is inspired by the proof of Theorem 1 of Rothman et al. (2008). Here we work with the penalized negative log-likelihood $Q_n(\Theta) = -pl_n(\Theta)$. Let $\Delta = \Theta - \Theta_0$, and define $G(\Delta) = Q(\Theta_0 + \Delta) - Q(\Theta_0)$ which is a convex function of Δ . Also let $\widehat{\Delta}_n = \widehat{\Theta}_n - \Theta_0$, where $\widehat{\Theta}_n$ is the proposed weighted **glasso** estimator which minimizes $Q_n(\Theta)$ or equivalently $\widehat{\Delta}_n$ minimizes $G(\Delta)$. Then $G(\widehat{\Delta}_n) \leq G(\mathbf{0}) = 0$. Now if we take a closed bounded convex set \mathcal{C} which contains $\mathbf{0}$, and show that G is strictly positive everywhere on the boundary $\partial\mathcal{C}$, then it implies that G has its minimizer $\widehat{\Delta}_n$ inside \mathcal{C} since G is continuous and $G(\mathbf{0}) = 0$. Define the set

$$\mathcal{C} = \{\Delta : \Delta = \Delta^\top, \|\Delta\|_F^2 \leq Mr_n^2\}$$

with the boundary

$$\partial\mathcal{C} = \{\Delta : \Delta = \Delta^\top, \|\Delta\|_F^2 = Mr_n^2\},$$

where M is a positive constant and $r_n = \{(p_n + q_n)(\log p_n)/n\}^{1/2}$. Then we must show that $P(\inf_{\Delta \in \partial\mathcal{C}} G(\Delta) > 0) \rightarrow 1$, as $n \rightarrow \infty$. We proceed as follows.

Using (1) and (2), we have that

$$\begin{aligned} G(\Delta) &= Q(\Theta_0 + \Delta) - Q(\Theta_0) = -\log \det(\Theta_0 + \Delta) + \log \det(\Theta_0) + \text{tr}(S_n(\Theta_0 + \Delta)) - \text{tr}(S_n\Theta_0) \\ &\quad + \lambda_n \{\|W * (\Theta_0 + \Delta)\|_1 - \|W * \Theta_0\|_1\}. \end{aligned}$$

Now, using the Taylor expansion of $f(t) = \log \det(\Theta + t\Delta)$ and the fact that Δ, Σ_0 and Θ_0 are all symmetric matrices, we have

$$\log \det(\Theta_0 + \Delta) - \log \det(\Theta_0) = \text{tr}(\Sigma_0\Delta) - [\text{vec}(\Delta)]^\top \left\{ \int_0^1 (1-v)(\Theta_0 + v\Delta)^{-1} \otimes (\Theta_0 + v\Delta)^{-1} dv \right\} \text{vec}(\Delta),$$

where $\text{vec}(\Delta)$ is the vectorized version of the matrix Δ to match the multiplication. Thus,

$$\begin{aligned} G(\Delta) &= \text{tr}(\Delta(S_n - \Sigma_0)) + [\text{vec}(\Delta)]^\top \left\{ \int_0^1 (1-v)(\Theta_0 + v\Delta)^{-1} \otimes (\Theta_0 + v\Delta)^{-1} dv \right\} \text{vec}(\Delta) \\ &\quad + \lambda_n \{\|W * (\Theta_0 + \Delta)\|_1 - \|W * \Theta_0\|_1\} = \mathbf{I}_1 + \mathbf{I}_2 + \mathbf{I}_3. \end{aligned}$$

To show that $G(\Delta)$ is strictly positive on $\partial\mathcal{C}$, we need to bound the quantities $\mathbf{I}_1, \mathbf{I}_2$ and \mathbf{I}_3 . By the union sum inequality, the Cauchy-Schwartz inequality, and Lemma 1, there exist

positive constants C_1 and C_2 such that with probability tending to 1, as $n \rightarrow \infty$,

$$\begin{aligned}
-|\mathbf{I}_1| &= -\left| \text{tr}(\Delta(S_n - \Sigma_0)) \right| \geq -\left| \sum_{i \neq j}^{p_n} \Delta_{ij}(s_{ij} - \sigma_{ij}^0) \right| - \left| \sum_{i=1}^{p_n} \Delta_{ii}(s_{ii} - \sigma_{ii}^0) \right| \\
&\geq -\max_{i \neq j} |s_{ij} - \sigma_{ij}^0| \times \|\Delta^-\|_1 - \sqrt{p_n} \max_{1 \leq i \leq p_n} |s_{ii} - \sigma_{ii}^0| \times \|\Delta^+\|_F \\
&\geq -C_1 \left(\frac{\log p_n}{n} \right)^{1/2} \|\Delta^-\|_1 - C_2 \left(\frac{p_n \log p_n}{n} \right)^{1/2} \|\Delta^+\|_F \\
&\geq -C_1 \left(\frac{\log p_n}{n} \right)^{1/2} (\|\Delta_T^-\|_1 - \|\Delta_{T^c}^-\|_1) - C_2 \left(\frac{(p_n + q_n) \log p_n}{n} \right)^{1/2} \|\Delta^+\|_F.
\end{aligned} \tag{12}$$

Also, as in Rothman et al. (2008), we have that

$$\begin{aligned}
\phi_{\min} \left\{ \int_0^1 (1-v)(\Theta_0 + v\Delta)^{-1} \otimes (\Theta_0 + v\Delta)^{-1} dv \right\} &\geq \int_0^1 (1-v) \phi_{\min}^2 \{ (\Theta_0 + v\Delta)^{-1} \} dv \\
&\geq \frac{1}{2} \min_{0 \leq v \leq 1} \phi_{\min}^2 \{ (\Theta_0 + v\Delta)^{-1} \} \geq \frac{1}{2} \min \left\{ \phi_{\min}^2 \{ (\Theta_0 + \Delta)^{-1} \} : \Delta \in \mathcal{C} \right\} \\
&= \frac{1}{2} \min \left\{ \phi_{\max}^{-2} \{ (\Theta_0 + \Delta) \} : \Delta \in \mathcal{C} \right\} \geq \frac{1}{4\tau_2^2}
\end{aligned}$$

with probability tending to one, where the last inequality is due to the regularity Condition 1, and also the fact that for all $\|\Delta\| \in \mathcal{C}$, we have $\|\Delta\| \leq \|\Delta\| \leq Mr_n^2 = o(1)$, as $n \rightarrow \infty$.

Thus, using the above inequality, with probability tending to one, we have

$$|\mathbf{I}_2| = \left| [\text{vec}(\Delta)]^\top \left\{ \int_0^1 (1-v)(\Theta_0 + v\Delta)^{-1} \otimes (\Theta_0 + v\Delta)^{-1} dv \right\} \text{vec}(\Delta) \right| \geq \frac{1}{4\tau_2^2} \|\Delta\|_F^2. \tag{13}$$

Next, since the penalty is decomposable (Negahban et al., 2012), we have that

$$|\mathbf{I}_3| \geq \lambda_n (\|W * \Delta_{T^c}^-\|_1 - \|W * \Delta_T^-\|_1). \tag{14}$$

Therefore, using the fact that $\|\Delta_T^-\|_1 \leq \sqrt{q_n} \|\Delta^-\|_F \leq \sqrt{p_n + q_n} \|\Delta^-\|_F$, and (12)-(14), we find that for large n ,

$$\begin{aligned}
G(\Delta) &\geq \frac{\gamma}{4\tau_2^2} \|\Delta\|_F^2 - C_2 \left\{ \frac{(p_n + q_n) \log p_n}{n} \right\}^{1/2} \|\Delta^+\|_F + \left\{ \lambda_n \min_{(i,j) \in T^c} \tilde{w}_{ij} - C_1 \left(\frac{\log p_n}{n} \right)^{1/2} \right\} \|\Delta_{T^c}^-\|_1 \\
&\quad - \left\{ \lambda_n \max_{(i,j) \in T} \tilde{w}_{ij} + C_1 \left(\frac{\log p_n}{n} \right)^{1/2} \right\} \|\Delta_T^-\|_1 \\
&\geq \frac{\gamma}{4\tau_2^2} \|\Delta\|_F^2 - C_2 \left\{ \frac{(p_n + q_n) \log p_n}{n} \right\}^{1/2} \|\Delta^+\|_F - \left\{ \lambda_n \max_{(i,j) \in T} \tilde{w}_{ij} + C_1 \left(\frac{\log p_n}{n} \right)^{1/2} \right\} \|\Delta_T^-\|_1
\end{aligned}$$

for $\{(\log p_n)/n\}^{1/2} (\min_{(i,j) \in T^c} \tilde{w}_{ij})^{-1} = O_p(\lambda_n)$.

Now, using $\Delta = \Delta^+ + \Delta^-$, we have that

$$\begin{aligned}
G(\Delta) &\geq \left\{ \frac{\gamma}{4\tau_2^2} - \left[\lambda_n \max_{(i,j) \in T} \tilde{w}_{ij} + C_1 \left(\frac{\log p}{n} \right)^{1/2} \right] (p_n + q_n)^{1/2} \|\Delta^-\|_F^{-1} \right\} \|\Delta^-\|_F^2 \\
&+ \left\{ \frac{\gamma}{4\tau_2^2} - C_2 \left(\frac{(p_n + q_n) \log p_n}{n} \right)^{1/2} \|\Delta^+\|_F^{-1} \right\} \|\Delta^+\|_F^2 \\
&= \left\{ \frac{\gamma}{4\tau_2^2} - \left[\frac{\lambda_n \max_{(i,j) \in T} \tilde{w}_{ij}}{C_1 (\log p_n/n)^{1/2}} + 1 \right] C_1 \left(\frac{(p_n + q_n) \log p_n}{n} \right)^{1/2} \|\Delta^-\|_F^{-1} \right\} \|\Delta^-\|_F^2 \\
&+ \left\{ \frac{\gamma}{4\tau_2^2} - C_2 \left(\frac{(p_n + q_n) \log p_n}{n} \right)^{1/2} \|\Delta^+\|_F^{-1} \right\} \|\Delta^+\|_F^2.
\end{aligned}$$

Since $\lambda_n \max_{(i,j) \in T} \tilde{w}_{ij} = O_p(\{(\log p_n)/n\}^{1/2})$, then on the boundary $\partial\mathcal{C}$, where $\|\Delta\|_F^2 = Mr_n^2$ with $r_n = \{(p_n + q_n)(\log p_n)/n\}^{1/2}$, we have that

$$G(\Delta) \geq \|\Delta^-\|_F^2 \left(\frac{\gamma}{4\tau_2^2} - C_1/\sqrt{M} \right) + \|\Delta^+\|_F^2 \left(\frac{\gamma}{4\tau_2^2} - C_2/\sqrt{M} \right).$$

Thus, for M sufficiently large, we have that $G(\Delta) > 0$ for any $\Delta \in \partial\mathcal{C}$, which completes the proof. ■

The result of the following Lemma is used for proving Theorem 2. First, we introduce some notation. We write the precision matrix Θ_0 as a $p_n(p_n + 1)/2$ -dimensional vector $\boldsymbol{\psi}_0$ by taking $\boldsymbol{\psi}_0 := \boldsymbol{\psi}_0(\Theta_0) = (\boldsymbol{\psi}_{01}, \boldsymbol{\psi}_{02})$ such that $\boldsymbol{\psi}_{02} = \mathbf{0}$. A similar presentation is used for any precision matrix Θ : $\boldsymbol{\psi} = \boldsymbol{\psi}(\Theta) = (\boldsymbol{\psi}_1, \boldsymbol{\psi}_2)$. Recall $r_n = \{(p_n + q_n)(\log p_n)/n\}^{1/2}$.

Lemma 2 *For any precision matrix Θ such that*

$$\|\Theta - \Theta_0\|_F = O_p(r_n) \quad , \quad \|\Theta - \Theta_0\|^2 = O_p(\eta_n)$$

where $\eta_n \rightarrow 0$ as $n \rightarrow \infty$, if $\{\frac{\log p}{n} + \eta_n\} \{\min_{(i,j) \in T^c} \tilde{w}_{ij}\}^{-2} = O_P(\lambda_n^2)$, then

$$pl_n((\boldsymbol{\psi}_1, \boldsymbol{\psi}_2); \lambda_n) - pl_n((\boldsymbol{\psi}_1, \mathbf{0}); \lambda_n) < 0 \tag{15}$$

with probability tending to 1 as $n \rightarrow \infty$, where $\boldsymbol{\psi} = \boldsymbol{\psi}(\Theta) = (\boldsymbol{\psi}_1, \boldsymbol{\psi}_2)$.

Proof of Lemma 2: Recall the definition of the penalized log-likelihood in (2) and with the general weighted L_1 -penalty in (4). We have that

$$pl_n((\boldsymbol{\psi}_1, \boldsymbol{\psi}_2); \lambda_n) - pl_n((\boldsymbol{\psi}_1, \mathbf{0}); \lambda_n) = \{\ell_n((\boldsymbol{\psi}_1, \boldsymbol{\psi}_2)) - \ell_n((\boldsymbol{\psi}_1, \mathbf{0}))\} - \sum_{(i,j) \in T^c} \lambda_n \tilde{w}_{ij} |\theta_{ij}|. \quad (16)$$

We first analyze the difference in the log-likelihood part. By the Mean Value Theorem,

$$\ell_n((\boldsymbol{\psi}_1, \boldsymbol{\psi}_2)) - \ell_n((\boldsymbol{\psi}_1, \mathbf{0})) = \left[\frac{\partial \ell_n((\boldsymbol{\psi}_1, \boldsymbol{\xi}))}{\partial \boldsymbol{\psi}_2} \right]^\top \times \boldsymbol{\psi}_2, \quad (17)$$

where $\boldsymbol{\xi}$ is a vector between $\boldsymbol{\psi}_2$ and $\boldsymbol{\psi}_{02} = \mathbf{0}$ such that $\|\boldsymbol{\xi}\|_2 \leq \|\boldsymbol{\psi}_2\|_2$.

As in the proof of Theorem 2 of Lam and Fan (2009), we have that

$$\frac{\partial \ell_n((\boldsymbol{\psi}_1, \boldsymbol{\xi}))}{\partial \boldsymbol{\psi}_2} = \{\sigma_{ij}(\boldsymbol{\xi}) - s_{ij} : (i, j) \in T^c\}.$$

We need to assess the orders of $\sigma_{ij}(\boldsymbol{\xi}) - s_{ij}$ as $n \rightarrow \infty$. Note that

$$\sigma_{ij}(\boldsymbol{\xi}) - s_{ij} = (\sigma_{ij}(\boldsymbol{\xi}) - \sigma_{ij}^0) + (\sigma_{ij}^0 - s_{ij}).$$

By Lam and Fan (2009), $|\sigma_{ij} - \sigma_{ij}^0| \leq \|\boldsymbol{\Sigma} - \boldsymbol{\Sigma}_0\|$, which has the order

$$\|\boldsymbol{\Sigma} - \boldsymbol{\Sigma}_0\| = \|\boldsymbol{\Sigma}(\boldsymbol{\Theta} - \boldsymbol{\Theta}_0)\boldsymbol{\Sigma}_0\| \leq \|\boldsymbol{\Sigma}\| \|\boldsymbol{\Theta} - \boldsymbol{\Theta}_0\| \|\boldsymbol{\Sigma}_0\|$$

and $\|\boldsymbol{\Sigma}_0\| = O(1)$ by Condition 1. Also using that $\eta_n \rightarrow 0$ so that $\lambda_{\min}(\boldsymbol{\Theta} - \boldsymbol{\Theta}_0) = o(1)$ for $\|\boldsymbol{\Theta} - \boldsymbol{\Theta}_0\| = O(\eta_n^{1/2})$, we find

$$\|\boldsymbol{\Sigma}\| = \lambda_{\min}^{-1}(\boldsymbol{\Theta}) \leq \left[\lambda_{\min}(\boldsymbol{\Theta}_0) + \lambda_{\min}(\boldsymbol{\Theta} - \boldsymbol{\Theta}_0) \right]^{-1} = O(1)$$

and since $\|\boldsymbol{\Theta} - \boldsymbol{\Theta}_0\| = O(\eta_n^{1/2})$, we have that $|\sigma_{ij} - \sigma_{ij}^0| = O(\eta_n^{1/2})$.

Since $\sigma_{ij}(\boldsymbol{\xi})$ is between σ_{ij} and σ_{ij}^0 , $|\sigma_{ij}(\boldsymbol{\xi}) - \sigma_{ij}^0| = O(\eta_n^{1/2})$. Therefore,

$$\max_{(i,j) \in T^c} |\sigma_{ij}(\boldsymbol{\xi}) - s_{ij}| = O_p(|s_{ij} - \sigma_{ij}^0| + \eta_n^{1/2}) \quad (18)$$

as $n \rightarrow \infty$. On the other hand, by Lemma 1,

$$\max_{(i,j) \in T^c} |s_{ij} - \sigma_{ij}^0| = O_p \left\{ \left(\frac{\log p}{n} \right)^{1/2} \right\} \quad (19)$$

as $n \rightarrow \infty$. Equations (18) and (19) imply that, as $n \rightarrow \infty$,

$$\max_{(i,j) \in T^c} |\sigma_{ij}(\boldsymbol{\xi}) - s_{ij}| = O_p \left\{ \left(\frac{\log p}{n} \right)^{1/2} + \eta_n^{1/2} \right\}. \quad (20)$$

Going back to the log-likelihood difference in (17), it can be written as

$$\ell_n((\boldsymbol{\psi}_1, \boldsymbol{\psi}_2)) - \ell_n((\boldsymbol{\psi}_1, \mathbf{0})) = \sum_{(i,j) \in T^c} \{\sigma_{ij}(\boldsymbol{\xi}) - s_{ij}\} |\theta_{ij}|. \quad (21)$$

Replacing the order assessment (20) in (21), we have that

$$\begin{aligned} pl_n((\boldsymbol{\psi}_1, \boldsymbol{\psi}_2); \lambda_n) - pl_n((\boldsymbol{\psi}_1, \mathbf{0}); \lambda_n) &= \{\ell_n((\boldsymbol{\psi}_1, \boldsymbol{\psi}_2)) - \ell_n((\boldsymbol{\psi}_1, \mathbf{0}))\} - \sum_{(i,j) \in T^c} \lambda_n \tilde{w}_{ij} |\theta_{ij}| \\ &\leq \sum_{(i,j) \in T^c} \{O_p((\log p/n)^{1/2} + \eta_n^{1/2}) |\theta_{ij}| - \lambda_n \tilde{w}_{ij} |\theta_{ij}|\} \\ &= \sum_{(i,j) \in T^c} \{O_p((\log p/n)^{1/2} + \eta_n^{1/2}) - \lambda_n \tilde{w}_{ij}\} |\theta_{ij}| < 0 \end{aligned}$$

if $\lambda_n^2 > (\min_{(i,j) \in T^c} \tilde{w}_{ij})^{-2} \left(\frac{\log p}{n} + \eta_n \right)$, for large n . In other words, if $\left(\frac{\log p}{n} + \eta_n \right) \left\{ \min_{(i,j) \in T^c} \tilde{w}_{ij} \right\}^{-2} = O_p(\lambda_n^2)$, then with probability approaching 1, as $n \rightarrow \infty$,

$$pl_n((\boldsymbol{\psi}_1, \boldsymbol{\psi}_2); \lambda_n) - pl_n((\boldsymbol{\psi}_1, \mathbf{0}); \lambda_n) < 0$$

and this completes the proof. ■

The implication of Lemma 2 is that in the neighborhood (specified by the conditions of this Lemma) of the truth precision matrix, $\boldsymbol{\psi}_0 = (\boldsymbol{\psi}_{01}, \boldsymbol{\psi}_{02}) = (\boldsymbol{\psi}_{01}, \mathbf{0})$, the penalized log-likelihood function $pl((\boldsymbol{\psi}_1, \boldsymbol{\psi}_2); \lambda_n)$ is maximized only when $\boldsymbol{\psi}_2 = \mathbf{0}$. We now proceed to the proof of Theorem 2.

Proof of Theorem 2: Let $(\hat{\boldsymbol{\psi}}_{n1}, \mathbf{0})$ be the maximizer of $pl_n((\boldsymbol{\psi}_1, \mathbf{0}); \lambda_n)$ which is considered as a function of $\boldsymbol{\psi}_1$ only. Then in the neighbourhood

$$\begin{aligned} \|\Theta - \Theta_0\|_F &= O_p \left\{ \left(\frac{(p_n + q_n) \log p_n}{n} \right)^{1/2} \right\} \\ \|\Theta - \Theta_0\|^2 &= O_p(\eta_n), \end{aligned}$$

we have that, by Lemma 2,

$$\begin{aligned} pl_n((\boldsymbol{\psi}_1, \boldsymbol{\psi}_2); \lambda_n) - pl_n((\widehat{\boldsymbol{\psi}}_{n1}, \mathbf{0}); \lambda_n) &= \{pl_n((\boldsymbol{\psi}_1, \boldsymbol{\psi}_2); \lambda_n) - pl_n(\boldsymbol{\psi}_1, \mathbf{0}); \lambda_n)\} \\ &\quad + \{pl_n((\boldsymbol{\psi}_1, \mathbf{0}); \lambda_n) - pl_n((\widehat{\boldsymbol{\psi}}_{n1}, \mathbf{0}); \lambda_n)\} \\ &< 0 \end{aligned}$$

with probability tending to one as $n \rightarrow \infty$. Therefore, in the chosen neighbourhood of Θ_0 , the maximum of $pl_n((\boldsymbol{\psi}_1, \boldsymbol{\psi}_2); \lambda_n)$ indeed happens at $(\widehat{\boldsymbol{\psi}}_{n1}, \mathbf{0})$. ■

Proof of Proposition 1: Theorems 1 and 2 require choices of the tuning parameter λ_n and the (possibly random) weights \tilde{w}_{ij} that, as $n \rightarrow \infty$, satisfy conditions

$$\lambda_n \max_{(i,j) \in T} \tilde{w}_{ij} = O_p \left(\sqrt{\frac{\log p_n}{n}} \right) \quad (22)$$

$$\left(\frac{\log p_n}{n} \right)^{1/2} \left\{ \min_{(i,j) \in T^c} \tilde{w}_{ij} \right\}^{-1} = O_p(\lambda_n) \quad (23)$$

$$\eta_n \left\{ \min_{(i,j) \in T^c} \tilde{w}_{ij} \right\}^{-2} = O_p(\lambda_n^2), \quad (24)$$

where $\lambda_n, \eta_n \rightarrow 0$. We now verify these conditions for the suggested weights \tilde{w}_{ij} in (3) used in the hubs weighted graphical lasso (`hw.glasso`). Note that these weights are constructed based on the popular graphical lasso (`glasso`) estimator $\tilde{\Theta}_n$. By Rothman et al. (2008), we have that as $n \rightarrow \infty$,

$$\|\tilde{\Theta}_n - \Theta_0\|_F = O_p \left(\sqrt{\frac{(p_n + q_n) \log p_n}{n}} \right). \quad (25)$$

We start with (22). By the definitions of the weights in (3), we have

$$\begin{aligned} \lambda_n \max_{(i,j) \in T} \tilde{w}_{ij} &= \lambda_n \max_{(i,j) \in T} \tilde{w}_{ij} = \max_{(i,j) \in T} \frac{\lambda_n}{|\tilde{\theta}_{ij}|^{\gamma_1} \left\{ \|\tilde{\boldsymbol{\theta}}_{-i}\|_1 \cdot \|\tilde{\boldsymbol{\theta}}_{-j}\|_1 \right\}^{\gamma_2}} \\ &= \frac{\lambda_n}{\min_{(i,j) \in T} |\tilde{\theta}_{ij}|^{\gamma_1} \left\{ \|\tilde{\boldsymbol{\theta}}_{-i}\|_1 \|\tilde{\boldsymbol{\theta}}_{-j}\|_1 \right\}^{\gamma_2}} \leq \lambda_n C(\tau_3), \end{aligned}$$

where the last inequality is due to (25), the regularity Condition 2 and that $T \neq \emptyset$, and $C(\tau_3)$ is a function of τ_3 . Thus (22) is satisfied, if we choose λ_n as

$$\lambda_n = O \left(\sqrt{\frac{\log p_n}{n}} \right),$$

as required in the first part of (8) of the Proposition.

For (23)-(24), once again using (25), Condition 2, and that $T \neq \emptyset$, for large n ,

$$\begin{aligned} \left\{ \min_{(i,j) \in T^c} \tilde{w}_{ij} \right\}^{-1} &= \max_{(i,j) \in T^c} \left\{ |\tilde{\theta}_{ij}|^{\gamma_1} \left[\|\tilde{\boldsymbol{\theta}}_{-i}\|_1 \|\tilde{\boldsymbol{\theta}}_{-j}\|_1 \right]^{\gamma_2} \right\} \\ &= \xi_2(\tau_3) \max_{(i,j) \in T^c} |\tilde{\theta}_{ij}|^{\gamma_1} \leq \xi_2(\tau_3) \left\{ \sum_{(i,j) \in T^c} \tilde{\theta}_{ij}^2 \right\}^{\gamma_1/2} \\ &\leq \xi_2(\tau_3) \left\{ \frac{(p_n + q_n) \log p_n}{n} \right\}^{\gamma_1/2} \end{aligned}$$

for some constant $\xi_2(\tau_3) > 0$. Thus, to satisfy (23)-(24), and using the above inequality, it is sufficient to choose λ_n and η_n such that

$$\begin{aligned} \left(\frac{\log p_n}{n} \right)^{1/2} \left\{ \frac{(p_n + q_n) \log p_n}{n} \right\}^{\gamma_1/2} \lambda_n^{-1} &= O(1) \\ \sqrt{\eta_n} \left(\frac{(p_n + q_n) \log p_n}{n} \right)^{\gamma_1/2} \lambda_n^{-1} &= O(1) \end{aligned}$$

as required by (8) and (9) of the Proposition.

References

- Aitchison, J. (1981). A new approach to null correlations of proportions. *Journal of Mathematical Geology* 13, 175–189.
- Barabási, A.-L. and R. Albert (1999). Emergence of scaling in random networks. *Science* 286, 509–512.
- Bickel, P. J. and E. Levina (2008). Regularized estimation of large covariance matrices. *Annals of Statistics* 36, 199–227.
- Charbonnier, C., J. Chiquet, and C. Ambroise (2010). Weighed-Lasso for Structured Network Inference from Time Course Data. *Statistical Applications in Genetics and Molecular Biology* 9, 1544–6115.
- Fan, J., Y. Feng, and Y. Wu (2009). Network exploration via the Adaptive Lasso and SCAD Penalties. *The Annals of Applied Statistics* 3, 521–541.

- Fan, J. and R. Li (2001). Variable selection via nonconcave penalized likelihood and its oracle properties. *Journal of the American Statistical Association* 96, 1348–1360.
- Fan, J., Y. Liao, and H. Liu (2016). An overview on the estimation of large covariance and precision matrices. *Econometrics Journal* 19, 1–32.
- Faust, K., L. Lahti, D. Gonze, W. de Vos, and J. Raes (2015). Metagenomics meets time series analysis: unraveling microbial community dynamics. *Current Opinion in Microbiology* 25, 56–66.
- Friedman, J. and E. J. Alm (2012). Inferring correlation networks from genomic survey data. *PLoS Comput Biol.* 8(9), e1002687.
- Friedman, J., T. Hastie, and R. Tibshirani (2008). Sparse inverse covariance estimation with the graphical lasso. *Biostatistics* 9, 432–441.
- Gao, X., D. Q. Pu, Y. Wu, and H. Xu (2012). Tuning Parameter Selection for Penalized Likelihood Estimation of Gaussian Graphical Model. *Statistica Sinica* 22, 1123–1146.
- Gilbert, J. A., F. Meyer, J. Jansson, J. Gordon, N. Pace, J. Tiedje, R. Ley, N. Fierer, D. Field, N. Kyrpides, et al. (2010). The earth microbiome project: Meeting Report of the “1st EMP meeting on Sample Selection and Acquisition” at Argonne National Laboratory October 6th 2010. *Standards in Genomic Sciences* 3, 249.
- Hero, A. and B. Rajaratnam (2012). Hub discovery in partial correlation graphs. *IEEE Transactions on Information Theory* 58, 6064–6078.
- Kurtz, Z. D., C. L. Müller, E. R. Miraldi, D. R. Littman, M. J. Blaser, and R. A. Bonneau (2015). Sparse and compositionally robust inference of microbial ecological networks. *PLoS Comput Biol.* 11(5), e1004226.
- Lam, C. and J. Fan (2009). Sparsistency and rates of convergence in large covariance matrix estimation. *Annals of Statistics* 37, 4254–4278.

- Li, J., I. Nasidze, D. Quinque, M. Li, H.-P. Horz, C. André, R. M. Garriga, M. Halbwax, A. Fischer, and M. Stoneking (2013). The saliva microbiome of Pan and Homo. *BMC Microbiology* 13, 204.
- Liu, Q. and A. Ihler (2011). Learning Scale Free Networks by Reweighted L1 Regularization. *Proceedings of the 14th International Conference on Artificial Intelligence and Statistics* 15, 40–48.
- Meinshausen, N. and P. Bühlmann (2006). High dimensional graphs and variable selection with the lasso. *Annals of Statistics* 34, 1436–1462.
- Negahban, S. N., P. Ravikumar, M. J. Wainwright, and B. Yu (2012). A unified framework for high-dimensional analysis of m-estimators with decomposable regularizers. *Statist. Sci.* 27, 538–557.
- Rothman, A., P. J. Bickel, E. Levina, and J. Zhu (2008). Sparse permutation invariant covariance estimation. *Electronic Journal of Statistics* 2, 494–515.
- Shen, X., W. Pan, and Y. Zhu (2012). Likelihood-based selection and sharp parameter estimation. *Journal of the American Statistical Association* 107, 223–232.
- Tan, K. M., P. London, K. Mohan, S.-I. Lee, M. Fazel, and D. Witten (2014). Learning Graphical Models with Hubs. *Journal of Machine Learning Research* 15, 3297–3331.
- Turnbaugh, P. J., R. E. Ley, M. Hamady, C. M. Fraser-Liggett, R. Knight, and J. I. Gordon (2007). The Human Microbiome Project. *Nature* 449, 804–810.
- van der Heijden, M. G. A. and M. Hartmann (2016). Networking in the plant microbiome. *PLoS Biol.* 14, 1–9.
- Yuan, M. and Y. Lin (2007). Model selection and estimation in the gaussian graphical model. *Biometrika* 94, 19–35.

Zou, H. (2006). The adaptive lasso and its oracle properties. *Journal of the American Statistical Association* 101, 1418–1429.

Method	True Pos. Rate (TPR)	True Neg. Rate (TNR)	Perc. of Correctly Estimated Hub Edges	Perc. of Correctly Estimated Hub / Non-Hub Nodes	Number of Estimated Edges	Frobenius Norm
<i>Simulation (i)</i>						
$n = 100, p = 50$						
glasso	72.69 (0.26)	84.03 (0.51)	61.27 (0.41)	100 (0)/32.85 (2.01)	234.71 (6.01)	3.30 (0.02)
Ada-glasso	80.51 (0.55)	96.40 (0.24)	74.51 (0.86)	100 (0)/88.65 (1.38)	105.87 (3.37)	1.73 (0.02)
SF	72.98 (0.27)	95.56 (0.18)	62.95 (0.42)	100 (0)/75.48 (1.09)	104.57 (2.25)	2.22 (0.02)
HGL ($c = 0.50$)	74.05 (0.22)	82.74 (0.40)	63.53 (0.36)	100 (0)/32.60 (1.53)	251.26 (4.73)	3.24 (0.02)
HGL ($c = 0.75$)	73.60 (0.19)	84.20 (0.24)	62.98 (0.32)	100 (0)/39.31 (0.80)	234.06 (2.82)	3.31 (0.02)
hw.glasso	87.06 (0.37)	98.67 (0.09)	85.85 (0.61)	100 (0)/99.33 (0.16)	89.52 (1.34)	1.14 (0.02)
2-step hw.glasso	94.27 (0.16)	98.49 (0.15)	98.51 (0.28)	100 (0)/99.33 (0.16)	101.87 (1.59)	0.94 (0.03)
2-step hw.glasso (known hubs)	94.57 (0.08)	99.20 (0.02)	99.08 (0.13)	100 (0)/100 (0)	94.29 (0.26)	0.79 (0.01)
$n = 100, p = 100$						
glasso	48.10 (0.26)	94.40 (0.28)	38.28 (0.33)	99.50 (0.35) / 73.70 (1.60)	384.73 (13.73)	7.29 (0.05)
Ada-glasso	58.31 (0.19)	96.55 (0.03)	52.97 (0.26)	100 (0) / 99.24 (0.10)	334.78 (1.42)	4.49 (0.02)
SF	53.08 (0.33)	97.94 (0.07)	46.53 (0.46)	99.25 (0.56) / 95.05 (0.37)	246.59 (4.50)	5.34 (0.04)
HGL ($c = 0.50$)	56.12 (0.17)	84.26 (0.29)	47.45 (0.20)	100 (0) / 19.91 (1.51)	886.60 (13.72)	6.43 (0.02)
HGL ($c = 0.75$)	50.81 (0.31)	92.82 (0.33)	42.05 (0.40)	99.50 (0.50) / 65.26 (1.67)	469.76 (16.53)	7.30 (0.04)
hw.glasso	70.55 (0.49)	99.60 (0.01)	72.77 (0.72)	100 (0) / 100 (0)	253.23 (2.68)	2.75 (0.03)
2-step hw.glasso	79.24 (0.36)	99.23 (0.01)	85.56 (0.52)	100 (0) / 100 (0)	311.58 (2.17)	2.62 (0.03)
2-step hw.glasso (known hubs)	79.24 (0.36)	99.23 (0.01)	85.56 (0.52)	100 (0) / 100 (0)	311.58 (2.17)	2.62 (0.03)
$n = 100, p = 200$						
glasso	24.76 (0.22)	99.30 (0.03)	16.01 (0.28)	66.38 (1.11) / 99.18 (0.11)	336.06 (9.93)	14.98 (0.09)
Ada-glasso	27.30 (0.13)	99.00 (0.03)	19.25 (0.16)	78.75 (0.91) / 99.99 (0.01)	432.65 (6.94)	13.28 (0.06)
SF	28.54 (0.14)	99.50 (0.02)	20.98 (0.17)	68.12 (0.86) / 99.81 (0.03)	361.03 (5.05)	11.19 (0.05)
HGL ($c = 0.50$)	49.69 (0.24)	58.26 (0.35)	41.73 (0.26)	100 (0) / 0 (0)	8319.62 (68.81)	73.08 (0.97)
HGL ($c = 0.75$)	33.69 (0.09)	92.95 (0.21)	26.28 (0.10)	93.12 (0.62) / 69.73 (1.29)	1654.97 (38.89)	13.14 (0.05)
hw.glasso	31.18 (0.16)	99.81 (0.01)	24.53 (0.21)	83.62 (1.11) / 100 (0)	347.32 (3.47)	8.91 (0.03)
2-step hw.glasso	42.15 (0.28)	99.69 (0.001)	38.75 (0.36)	83.62 (1.11) / 100 (0)	548.95 (5.10)	8.76 (0.04)
2-step hw.glasso (known hubs)	45.18 (0.18)	99.65 (0.005)	42.67 (0.23)	100 (0) / 100 (0)	605.59 (3.38)	8.76 (0.04)

Table 1: Means (and standard errors) of different performance measures over 100 replications for the graphical lasso (glasso), adaptive lasso (Ada-glasso), scale-free network approach (SF), hubs graphical lasso (HGL), hubs weighted graphical lasso (hw.glasso), and 2-step hw.glasso.

Method	True Pos. Rate (TPR)	True Neg. Rate (TNR)	Perc. of Correctly Estimated Hub Edges	Perc. of Correctly Estimated Hub / Non-Hub Nodes	Number of Estimated Edges	Frobenius Norm
<i>Simulation (ii)</i>						
$n = 100, p = 50$						
glasso	90.42 (0.25)	93.48 (0.15)	88.64 (0.31)	100 (0)/69.60 (0.65)	107.74 (1.87)	1.01 (0.01)
Ada-glasso	91.21 (0.27)	98.15 (0.11)	93.00 (0.50)	100 (0)/99.17 (0.14)	53.18 (1.45)	0.51 (0.01)
SF	87.83 (0.22)	97.59 (0.08)	90.43 (0.32)	100 (0)/92.31 (0.52)	56.79 (1.05)	0.65 (0.01)
HGL ($c = 0.50$)	91.27 (0.24)	92.17 (0.24)	89.75 (0.31)	100 (0)/64.83 (1.05)	124.10 (2.96)	1.01 (0.01)
HGL ($c = 0.75$)	90.34 (0.23)	93.19 (0.13)	89.29 (0.29)	100 (0)/68.77 (0.63)	111.15 (1.57)	1.04 (0.01)
hw.glasso	91.48 (0.25)	98.47 (0.07)	94.68 (0.40)	100 (0)/99.50 (0.10)	49.55 (0.96)	0.46 (0.01)
2-step hw.glasso	87.65 (0.17)	96.92 (0.07)	96.68 (0.31)	100 (0)/99.50 (0.10)	64.59 (0.81)	0.52 (0.01)
2-step hw.glasso (known hubs)	87.21 (0.15)	97.17 (0.05)	96.57 (0.28)	100 (0)/100 (0)	61.23 (0.65)	0.51 (0.01)
$n = 100, p = 100$						
glasso	66.17 (0.36)	97.48 (0.07)	57.84 (0.62)	99.25 (0.43) / 92.75 (0.35)	198.98 (4.25)	2.54 (0.01)
Ada-glasso	72.86 (0.19)	98.57 (0.02)	72.56 (0.37)	99.75 (0.25) / 100 (0)	164.85 (0.92)	1.59 (0.01)
SF	71.31 (0.26)	98.38 (0.04)	72.86 (0.47)	100 (0) / 97.74 (0.15)	169.79 (2.34)	1.77 (0.01)
HGL ($c = 0.50$)	74.01 (0.27)	94.27 (0.16)	69.57 (0.39)	100 (0) / 76.81 (0.84)	373.57 (8.07)	2.32 (0.01)
HGL ($c = 0.75$)	68.34 (0.33)	96.87 (0.09)	62.33 (0.54)	100 (0) / 88.56 (0.49)	234.09 (5.24)	2.52 (0.01)
hw.glasso	74.94 (0.24)	99.11 (0.03)	83.49 (0.42)	100 (0) / 100 (0)	144.86 (1.77)	1.25 (0.01)
2-step hw.glasso	75.02 (0.16)	97.83 (0.03)	88.98 (0.36)	100 (0) / 100 (0)	206.12 (1.93)	1.44 (0.01)
2-step hw.glasso (known hubs)	75.02 (0.16)	97.83 (0.03)	88.98 (0.36)	100 (0) / 100 (0)	206.12 (1.93)	1.44 (0.01)
$n = 100, p = 200$						
glasso	36.77 (0.24)	99.47 (0.02)	23.10 (0.38)	48.00 (1.27) / 99.79 (0.03)	222.39 (6.03)	5.71 (0.02)
Ada-glasso	41.83 (0.21)	99.30 (0.03)	31.27 (0.33)	60.25 (1.26) / 100 (0)	299.40 (6.88)	5.17 (0.02)
SF	43.25 (0.22)	99.39 (0.02)	34.32 (0.35)	68.38 (1.01) / 99.72 (0.03)	294.44 (4.61)	4.47 (0.02)
HGL ($c = 0.50$)	73.53 (0.21)	57.97 (0.31)	66.61 (0.27)	100 (0) / 0 (0)	8522.47 (61.84)	30.42 (0.41)
HGL ($c = 0.75$)	49.11 (0.22)	96.56 (0.10)	41.35 (0.28)	92.25 (0.94) / 92.83 (0.43)	888.32 (21.62)	5.13 (0.02)
hw.glasso	50.98 (0.29)	99.51 (0.01)	47.95 (0.47)	85.88 (0.98) / 100 (0)	338.71 (4.53)	3.43 (0.02)
2-step hw.glasso	56.55 (0.30)	98.95 (0.02)	58.04 (0.53)	85.88 (0.98) / 100 (0)	493.88 (5.16)	3.75 (0.02)
2-step hw.glasso (known hubs)	58.80 (0.26)	98.92 (0.02)	61.92 (0.46)	100 (0) / 100 (0)	519.27 (5.20)	3.76 (0.02)

Table 2: Means (and standard errors) of different performance measures over 100 replications for the graphical lasso (glasso), adaptive lasso (Ada-glasso), scale-free network approach (SF), hubs graphical lasso (HGL), hubs weighted graphical lasso (hw.glasso), and 2-step hw.glasso.

Method	True Pos. Rate (TPR)	True Neg. Rate (TNR)	Perc. of Correctly Estimated Hub Edges	Perc. of Correctly Estimated Hub / Non-Hub Nodes	Number of Estimated Edges	Frobenius Norm
<i>Simulation (iii)</i>						
$n = 100, p = 50$						
glasso	90.43 (0.27)	89.16 (0.25)	95.03 (0.39)	100 (0)/46.44 (1.33)	178.92 (3.12)	1.52 (0.01)
Ada-glasso	87.93 (0.23)	97.21 (0.04)	95.74 (0.32)	100 (0)/96.58 (0.28)	82.67 (0.58)	0.80 (0.01)
SF	86.44 (0.27)	95.93 (0.11)	95.47 (0.37)	100 (0)/79.56 (0.80)	95.76 (1.54)	1.03 (0.01)
HGL ($c = 0.50$)	89.61 (0.25)	89.39 (0.24)	94.74 (0.37)	100 (0)/50.40 (1.13)	175.31 (2.94)	1.60 (0.01)
HGL ($c = 0.75$)	88.78 (0.20)	90.47 (0.13)	94.37 (0.36)	100 (0)/56.21 (0.56)	161.84 (1.66)	1.67 (0.01)
hw.glasso	87.30 (0.31)	97.67 (0.11)	96.21 (0.32)	100 (0)/96.92 (0.45)	76.53 (1.53)	0.78 (0.01)
2-step hw.glasso	79.92 (0.33)	95.61 (0.20)	98.95 (0.18)	100 (0)/96.15 (0.64)	92.09 (2.63)	0.94 (0.01)
2-step hw.glasso (known hubs)	78.03 (0.16)	97.14 (0.05)	99.92 (0.05)	100 (0)/100 (0)	72.16 (0.65)	0.88 (0.01)
$n = 100, p = 100$						
glasso	51.91 (0.30)	97.41 (0.06)	42.35 (0.46)	66.50 (1.95) / 87.89 (0.37)	199.94 (3.78)	3.57 (0.02)
Ada-glasso	49.45 (0.33)	99.59 (0.03)	43.01 (0.58)	68.50 (1.80) / 99.99 (0.01)	88.70 (2.18)	2.54 (0.01)
SF	49.10 (0.41)	98.76 (0.04)	39.98 (0.80)	64.50 (1.92) / 97.00 (0.22)	126.91 (3.14)	2.79 (0.02)
HGL ($c = 0.50$)	57.68 (0.29)	95.55 (0.10)	53.82 (0.46)	95.25 (1.11) / 79.58 (0.48)	307.45 (5.35)	3.45 (0.01)
HGL ($c = 0.75$)	52.01 (0.49)	96.90 (0.10)	43.84 (0.82)	75.75 (2.29) / 85.84 (0.47)	224.18 (6.07)	3.64 (0.02)
hw.glasso	57.97 (0.34)	99.31 (0.03)	63.07 (0.63)	95.25 (0.99) / 99.99 (0.01)	131.19 (2.34)	2.10 (0.01)
2-step hw.glasso	61.46 (0.35)	98.77 (0.04)	75.27 (0.82)	95.25 (0.99) / 99.99 (0.01)	168.87 (2.68)	2.31 (0.02)
2-step hw.glasso (known hubs)	62.65 (0.26)	98.76 (0.04)	78.07 (0.61)	100 (0) / 100 (0)	173.14 (2.53)	2.30 (0.02)
$n = 100, p = 200$						
glasso	33.57 (0.23)	99.04 (0.04)	30.07 (0.36)	65.38 (0.75) / 99.74 (0.05)	392.68 (9.40)	8.87 (0.03)
Ada-glasso	36.13 (0.14)	99.13 (0.03)	34.70 (0.21)	69.12 (1.07) / 100 (0)	405.32 (6.17)	6.99 (0.02)
SF	35.82 (0.14)	99.46 (0.02)	35.89 (0.23)	67.25 (0.68) / 99.97 (0.01)	340.27 (4.27)	6.73 (0.02)
HGL ($c = 0.50$)	42.27 (0.10)	95.90 (0.09)	40.85 (0.20)	82.00 (0.74) / 92.01 (0.32)	1091.75 (17.25)	7.87 (0.02)
HGL ($c = 0.75$)	42.34 (0.07)	95.69 (0.03)	40.50 (0.12)	82.25 (0.69) / 91.79 (0.29)	1130.89 (6.53)	7.82 (0.02)
hw.glasso	37.78 (0.17)	99.66 (0.01)	41.03 (0.32)	76.62 (1.25) / 100 (0)	325.78 (3.59)	5.37 (0.02)
2-step hw.glasso	43.17 (0.30)	99.26 (0.02)	51.72 (0.58)	76.62 (1.25) / 100 (0)	467.41 (5.80)	5.72 (0.03)
2-step hw.glasso (known hubs)	47.59 (0.15)	99.25 (0.01)	60.26 (0.29)	100 (0) / 100 (0)	524.46 (4.29)	5.68 (0.03)

Table 3: Means (and standard errors) of different performance measures over 100 replications for the graphical lasso (glasso), adaptive lasso (Ada-glasso), scale-free network approach (SF), hubs graphical lasso (HGL), hubs weighted graphical lasso (hw.glasso), and 2-step hw.glasso.

Method	True Pos. Rate (TPR)	True Neg. Rate (TNR)	Perc. of Correctly Estimated Hub Edges	Perc. of Correctly Estimated Hub / Non-Hub Nodes	Number of Estimated Edges	Frobenius Norm
<i>Simulation (iv)</i>						
$n = 100, p = 50$						
glasso	88.83 (0.41)	90.34 (0.30)	95.62 (0.42)	100 (0)/56.75 (1.26)	151.50 (3.83)	1.28 (0.01)
Ada-glasso	89.79 (0.29)	97.51 (0.08)	95.31 (0.37)	100 (0)/98.85 (0.16)	68.15 (1.05)	0.60 (0.01)
SF	83.71 (0.27)	97.10 (0.10)	95.31 (0.47)	99.50 (0.50)/93.79 (0.60)	67.01 (1.33)	0.83 (0.01)
hw.glasso	87.22 (0.30)	98.52 (0.07)	95.22 (0.41)	100 (0)/99.73 (0.08)	53.74 (0.99)	0.55 (0.01)
2-step hw.glasso	83.84 (0.18)	96.51 (0.06)	99.31 (0.13)	100 (0)/99.71 (0.08)	74.10 (0.80)	0.62 (0.01)
2-step hw.glasso (known hubs)	83.32 (0.16)	96.64 (0.05)	99.12 (0.14)	100 (0)/100 (0)	71.97 (0.63)	0.62 (0.01)
$n = 100, p = 100$						
glasso	70.58 (0.31)	98.34 (0.08)	64.92 (0.84)	83.00 (2.39) / 97.04 (0.43)	121.01 (4.38)	1.57 (0.01)
Ada-glasso	78.69 (0.35)	98.85 (0.06)	80.29 (0.71)	79.00 (2.71) / 99.99 (0.01)	112.62 (3.28)	0.91 (0.01)
SF	72.25 (0.32)	99.27 (0.03)	72.19 (0.98)	71.00 (2.67) / 99.96 (0.03)	79.14 (2.04)	1.10 (0.01)
hw.glasso	76.94 (0.27)	99.29 (0.03)	80.53 (0.67)	80.00 (2.22) / 100 (0)	87.66 (1.64)	1.03 (0.01)
2-step hw.glasso	75.01 (0.46)	98.29 (0.03)	83.10 (1.55)	80.33 (2.23) / 100 (0)	132.03 (2.35)	0.92 (0.01)
2-step hw.glasso (known hubs)	79.01 (0.08)	98.08 (0.03)	96.58 (0.22)	100 (0) / 100 (0)	150.42 (1.35)	0.88 (0.01)
$n = 100, p = 200$						
glasso	64.25 (0.18)	99.64 (0.01)	63.59 (0.75)	52.33 (1.66) / 100 (0)	128.12 (3.53)	1.50 (0.01)
Ada-glasso	70.13 (0.29)	99.64 (0.03)	80.73 (0.64)	62.67 (2.69) / 100 (0)	150.55 (6.42)	1.08 (0.01)
SF	67.81 (0.18)	99.74 (0.01)	81.60 (0.79)	80.67 (1.85) / 100 (0)	122.53 (2.33)	1.15 (0.01)
hw.glasso	69.47 (0.14)	99.75 (0.01)	86.45 (0.45)	87.33 (1.63) / 100 (0)	127.06 (1.74)	0.96 (0.01)
2-step hw.glasso	68.85 (0.27)	99.41 (0.01)	87.81 (1.27)	88.33 (1.60) / 100 (0)	191.34 (2.63)	1.07 (0.01)
2-step hw.glasso (known hubs)	70.79 (0.05)	99.39 (0.01)	96.86 (0.20)	100 (0) / 100 (0)	202.21 (2.38)	1.05 (0.01)

Table 4: Means (and standard errors) of different performance measures over 100 replications for the graphical lasso (glasso), adaptive lasso (Ada-glasso), scale-free network approach (SF), hubs weighted graphical lasso (hw.glasso), and 2-step hw.glasso.

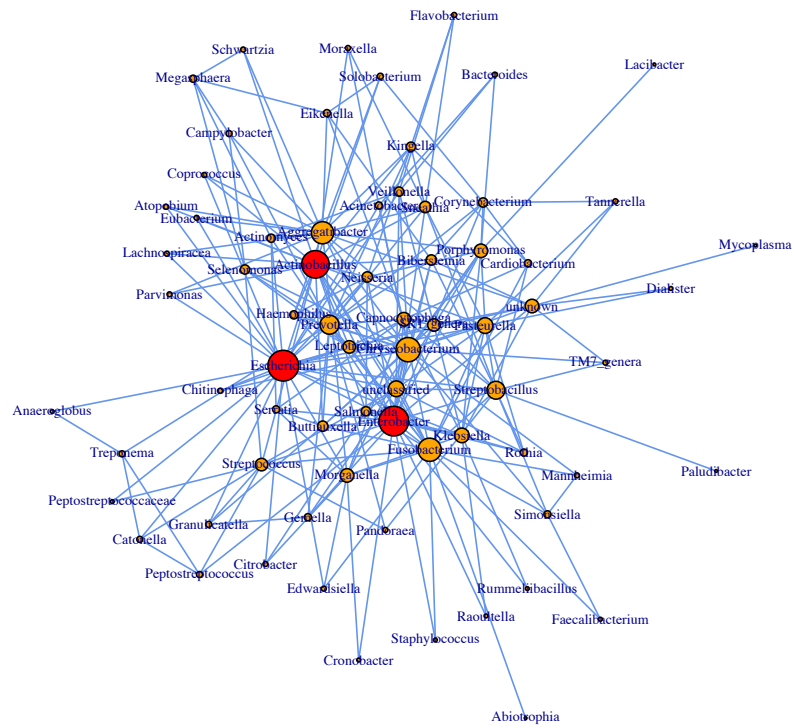


Figure 2: Bonobo microbial interaction network, estimated by the hubs weighted graphical lasso.

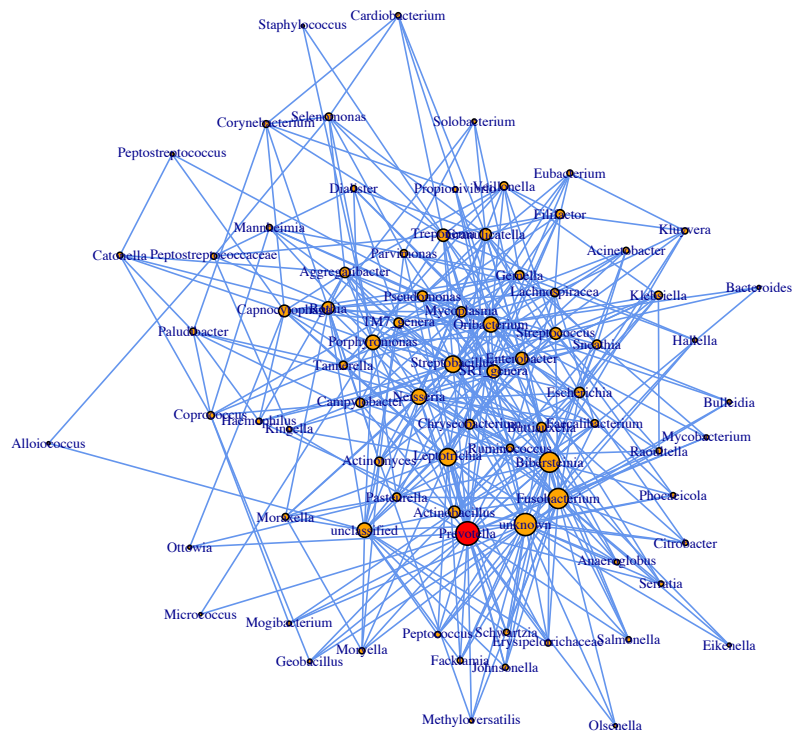


Figure 3: Chimpanzee microbial interaction network, estimated by the hubs weighted graphical lasso.